Bandwidth of MFL in steel plate inspection

Neil R. PEARSON[1], Matthew A. BOAT[1], John S. D. MASON[2]
Contact: [1]Silverwing UK Ltd; Clos Llyn Cwm,
Swansea Enterprise Park, Swansea, SA6 8QY, UK
[2]College of Engineering, Swansea University Bay Campus,
Fabian Way, Swansea, SA1 8EN, UK.

e-mail: npearson@silverwingndt.com

Abstract. Magnetic flux leakage (MFL) continues to be a widely used approach to detect defects caused by corrosion in applications with large areas. The principal merit of MFL is that large areas can be covered relatively quickly making it beneficial for example in the inspection of asset components that are costly to expose and in large area; two good examples are the floor of above ground storage tanks or exceedingly large surface areas such as pipelines. Though rapid, MFL is continually reported to have limitations when estimating the geometry of defects. In this paper we introduce and define the frequency response (FR) of MFL in an attempt to understand the relationship between MFL and defect geometry. This novel approach describes the relationship between MFL and defect shape using simulated sinusoidal defects to reveal important fundamental characteristics of MFL.

Keywords:
Magnetic flux leakage (MFL), defect reconstruction , MFL frequency response (FR), MFL bandwidth

Introduction

Magnetic flux leakage (MFL) is a common non-destructive testing (NDT) approach and is often employed to detect and map material loss on ferrous steel structures. Its principal advantage over other forms of NDT is its ability to inspect large areas quickly. These areas can be hundreds of m^2, requiring the MFL tool to find and ideally determine the size of any material loss with diameters in the region of *mm*'s. Regions of material loss are normally referred to as 'defects' and are usually a consequence of corrosion. To facilitate appropriate repair and keep these steel structures in-service for as long as possible, defects not only need to be located but also their profiles estimated. In its current form, MFL is seen as being somewhat unreliable in providing a defect's profile or basic geometries. Furthermore, MFL is known to miss certain defects altogether. Thus when estimating the profile of a defect from a corresponding MFL signal, there is an inherent ambiguity as reported in [1, 2]. This ambiguity means that the true nature of the defect remains unknown, drawing into question any subsequent repair strategy and thus the future integrity of the asset. Such ambiguity has been addressed many times in the literature and particularly in the works of [2, 3]; it is reported that defects with very different surface profiles can give rise to two very similar MFL signals. This implies that the information necessary to discriminate between defects has limitations and these limitations need to be understood.

In this paper a new forward model of the MFL system is presented that is able to characterise all conditions under which defect representations could compromised, for example, the omission of certain geometric details. This new forward model has been formulated under the postulation that a cross-sectional profile of any defect can be constructed from one or more sinusoids of particular frequencies, amplitudes and phases. Studying the amplitude of MFL signals from defects synthesised from the weighted sum of selected sinusoids exposes some of the principal and as yet unexplained characteristics of the relationship between MFL and surface defects.

The principle finding of this work is a measure of the system bandwidth. In the context of MFL the associated band-limits provide a means to classify the level of MFL ambiguity. From these findings, it is postulated that any defect profile can be decomposed to reveal its fundamental characteristics of MFL including the sources of previously reported ambiguities.

1. Defect classification in the frequency domain

Any time-varying signal can be broken down into a set of spectral components; audio signals are one such example. Similarly, a spatial domain signal, like a defect profile can too be represented by a set of spatial frequencies. In this paper, a single spatial frequency is simply referred to as 'frequency' (f), defined as the number of cycles per metre (c/m).

The frequency components required to construct any defect can be thought of as residing between two limits; namely the upper and lower cut-off frequencies. In the context of defects, the upper cut-off frequency relates to fine detail and hereby denoted $f_H(DS)$. Conversely, the lower cut-off frequency would relate to defects with large area loss and maybe large material loss. It can also be thought that this cut-off relates to the threshold between large defects caused by corrosion and those caused by erosion. This lower cut-off is referred to by $f_L(DS)$. Both $f_L(DS)$ and $f_H(DS)$ define the bandwidth of 'defect space' (DS), which is a continuum where it is possible to define any defect profile via a particular combination of amplitude weighted frequency components. This is illustrated in Figure 1.(i), to represent the spectral range and poential weighting of components, normalised here between zero and one.

Ideally, an MFL signal would give a true representation of a defect profile, however, in reality, the system will have a frequency response, a weighting scheme that will impact on the amplitude or phase of the original defect spectral components. Thus the resulting MFL signal is an altered representation of the original defect profile. The weighting scheme of the system is a step towards describing the MFL forward model and if known, then it may be possible to recover the original defect weightings and hence its profile. This is the primary focus of this paper, the derivation of the MFL forward model of amplitude weightings, achieved through a frequency response approach.

For illustration, consider the simple weighting envelope shown in Figure 1.(ii) to represent the frequency response of an MFL system. Similarly to the band-limits that define defect space, the range of frequencies that reflect the capability of MFL can also be defined by two band-limits. These limits can be established by locating a threshold at a particular level that intersects with the MFL weighting envelope, i.e. its frequency response (FR). The threshold level is subjective and can be selected by, for example, ascertaining the sensitivity of an acquisition system (e.g. the quantisation of the ADC). A conventional $-3\ dB$ level is chosen for this narration resulting in two band-limits denoted $f_L(MFL)$ and $f_H(MFL)$. $f_L(MFL)$ corresponds to the lowest frequency component of defects that can be represented in an MFL signal (those with large periods of hundreds of $mm's$). The upper limit of MFL signal space,

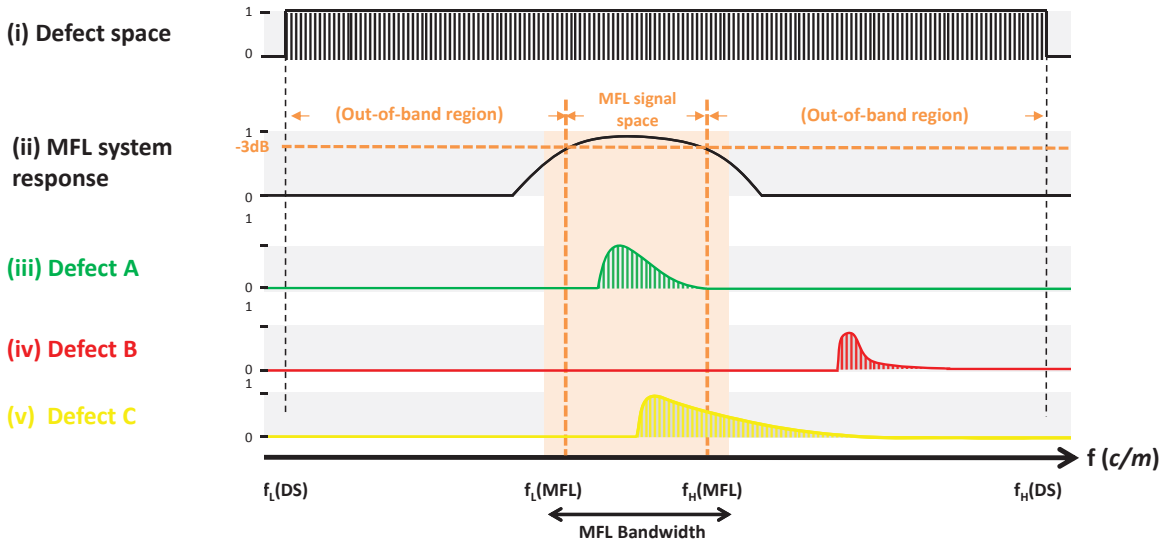

Fig. 1. Bandwidth of MFL within defect space. Spatial frequency is represented by the number of defect cycles per metre (c/m), on the abscissa. Defect space is defined by $f_L(DS)$ and $f_H(DS)$, 'MFL signal space' is defined by $f_L(MFL)$ and $f_H(MFL)$ and three defects, A, B and C are used to illustrate the potential class of defects, namely in-band, out-of-band and across-band respectively.

$f_H(MFL)$, represents the smallest defect components that can be found by MFL (geometries in the region of $mm's$). Thus, any components of a defect above $f_H(MFL)$ and any defect component below $f_L(MFL)$ would not be present in the corresponding MFL signal and are in the out-of-band region of MFL. The region between $f_L(MFL)$ and $f_H(MFL)$ defines the in-band components, defining 'MFL signal space'.

1.1 Defect classes

As MFL has been shown to be unable to reflect all the geometries of a defect, the band-limits of defect space and MFL signal space are unlikely to coincide. Though not realising it, the early work of Ramirez [4] indicated the region of $f_H(MFL)$ when the author reported that narrow and deep defects are the most difficult to find via MFL because MFL signals coming 'from' smaller defects tended to look the same. The original findings of Ramirez imply that in the context of MFL signal space, $f_H(MFL)$ represents the inherent limitation of MFL. It can then be postulated that limits $f_L(MFL)$ and $f_H(MFL)$ cover a subregion of DS and exist between the outer limits of $f_L(DS)$ and $f_H(DS)$, as shown by the narrow frequency range of MFL signal space in Figure 1.(ii).

As a defect profile can be constructed from one or more sinusoids and that MFL signal space is postulated to exist within defect space, then the MFL band-limits can be used to classify **any** defect into one of three categories:

Wholly in-band: The defect class where all components of a profile exist between the band-limits $f_L(MFL)$ and $f_H(MFL)$. All defect components are reflected in the corresponding MFL signal. This is the ideal case as no defect information is missing and so an accurate representation of the original defect profile might well be possible. **Defect A** in Figure 1.(iii) illustrates an in-band defect with all defect components between the

two MFL band-limits. A true representation of the defect profile in this instance is possible only if the frequency weighting of the MFL system is known (i.e. the MFL FR shape).

Wholly out-of-band: Here, a defect has **all** of its components outside the MFL band-limits. The spectral components have become so heavily attenuated by the MFL system that they are out of the range, e.g. a narrow pit just *mm*'s in diameter can be missed for this reason, especially if it is shallow. **Defect B** in Figure 1.(iv) is shown to be outside the band-limits of MFL meaning that it would not be detected.

Across-band: The final defect category represents defect that has both 'in-band' and 'out-of-band' components. While in-band components are reflected in the MFL signal, the out-of-band components are attenuated to such an extent that they are not reflected in the signal. This means that the representation is poor. $f_H(MFL)$ is shown to cut through the frequency make-up of **Defect C** in Figure 1.(v). In this example, the in-band components of Defect C would be reflected, though convolved with the additional attenuation of the MFL system response. The components outside the bandwidth are attenuated to such an extent that they are not reflected in the MFL signal. Thus any defect with both in-band and out-of-band components (below $f_L(MFL)$ or above $f_H(MFL)$) is a condition for ambiguity in MFL.

Both the in-band and out-of-band cases require a defect to have at least one or more components, but the 'across-band' category requires at least two components. With at least one defect component out-of-band then any attempt to estimate the original profile of an across-band defect will always result in an error. If $f_L(MFL)$ could be somehow modified to tend towards $f_L(DS)$ and/or $f_H(MFL)$ increased towards $f_H(DS)$, then the error in a defects representation could be reduced.

The across-band class corresponds to observations made in the associated literature, for example [2–4], where two different defects have resulted in similar MFL signals. It can be thought that the across-band category represents the typical in-the-field case, because without knowing the true defect profile, an ambiguous outcome is all that can be assumed with MFL. This is true unless the MFL bandwidth can cover the entire operational range of defect space.

As MFL is known to be band-limited then any in-field defect should always be categorised as 'across-band' because the ground truth of the defect profile is not known. Though, if the bandwidth could be extended to encompass more defect space and cover the region of defects normally found on the surfaces of steel structures, then ambiguity is less likely to occur. Ultimately, if the MFL bandwidth were able to match that of the defect bandwidth, then no ambiguity would occur and all defects would be in-band. In the next section, example in-band and across-band defects and their corresponding signals are presented. An out-of-band defect example is omitted as there would simply be no MFL signal to interpret.

1.2 Example in-band and across-band defects

The band-limiting nature of MFL is now exemplified via three defects. One defect has a smooth conical shape while the others contain two vertical edges; referred to as a 'square' defect for simplicity. Each of these defects have the same peak depth and are shown on the top row in Figure 2. along with their corresponding MFL signals below; these signals have been obtained via simulation. Figure 2(a) represents a smoothed sinusoidal defect. The sinusoidal defect aims to demonstrate the MFL signal for a wholly in-band defect that comprises of a

single frequency component. This defect has a peak depth (δ_D) of 3 *mm* (i.e. '50 %' of the nominal plate thickness) and its length (δ_L) is 200 *mm*, measured from crest-to-crest. Though this may seem to be a rather large defect, it is possible to find corrosion with such geometries in the field. The corresponding MFL magnitude signal ($|B_{XZ}^{Leak}|$)[1] is seen to represent an exceedingly close approximation of the original defect profile. This implies that, under this condition in particular, MFL is capable of reflecting the true nature of a defect. Note that MFL signals tends to peak in the vicinity of the largest material loss, but for simple comparison to its corresponding defect profiles, $|B_{XZ}^{Leak}|$ has been inverted.

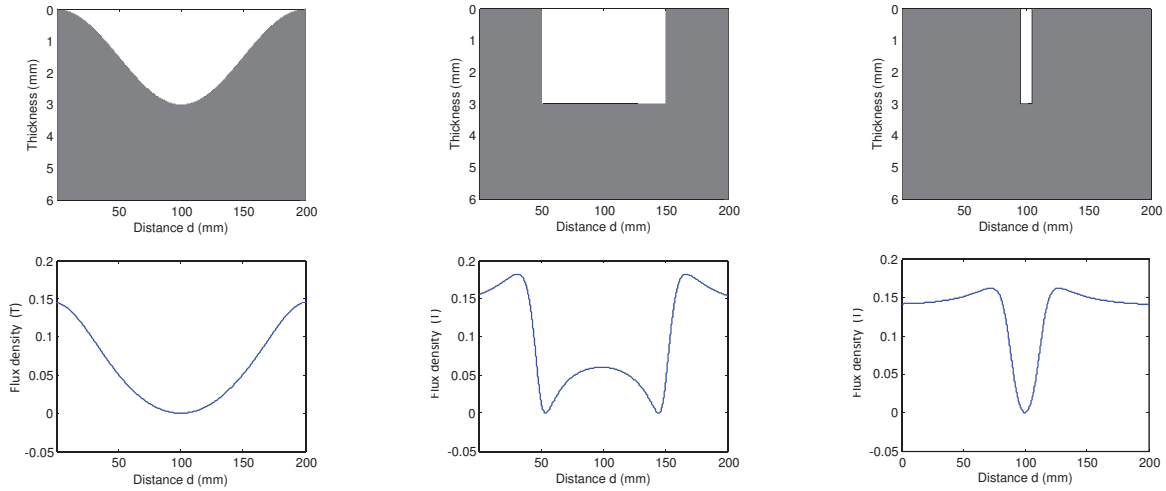

(a) A smooth sinusoidal defect that is considered **in-band**.

(b) Wide, 100 *mm* square shaped defect, categorised as **across-band**.

(c) Narrow, 10 *mm* square shaped defect, again categorised to be **across-band**.

Fig. 2. Three simulated example defects and their corresponding MFL signals ($|B_{XZ}^{Leak}|$) as a function of distance. These signals have been inverted and D.C. shifted to aid the comparison between the defect shape and the profile of the corresponding MFL signal.

Now consider the square shape defect in Figure 2(b) where again, δ_D is 50 % of the material thickness but this time δ_L is 100 *mm*. While δ_L for the smoothed conical and square defects differ, their period does not. This identical period of 200 *mm* for both examples in Figure 2(a) and 2(b) is intentional so that each defect contains the same material volume loss.

As commented by Saunderson [5], MFL signal amplitude is closely representative of material volume loss. Assuming this is true, the amplitudes of the corresponding MFL signals should be very similar. Though with these particular examples, the MFL amplitude for defects with the same volume is different, with the resulting signal amplitude of the wide square approximately 20 % greater than that of the sinusoid. Thus, for these defect examples, the correlation between volumetric material loss and signal amplitude does not hold.

So, let us investigate the defect shapes and their corresponding signals. It is clear that the sinusoidal defect and its MFL signal are very similar and based on the earlier classification

[1] The MFL signals presented in this paper is a magnitude measure from the X and Y signals that would normally be obtained with two separate magnetic sensors (Hall-effect or coils). The same measure is used to obtain the frequency response later in this paper.

scheme. This means that the defects components are likely to be in-band. Though representative, the shape of MFL signal for the square defect is distorted, implying that there are many components out-of-band. Of course, to obtain a vertical edge in the MFL signal, its bandwidth would have to be infinite but there is a degree of similarity that could be achieved with a band-limited system, though MFL appears to have a significant band-limitation with a number of components 'out-of-band'. Frequency components necessary to represent the defect via MFL have somehow been omitted or heavily attenuated out of the system capability. Though, with at least some indication of a defect because an MFL signal is present, the defect would be classed 'across-band'.

As the square defect is represented by a distorted MFL signal with different amplitudes and other characteristics. The gradient of the signal, corresponding to the vertical edges of the defect, is another indication of MFLs band-limitations. Now consider the smaller 'square' defect with a narrow δ_L shown in Figure 2(c). With the vertical edges of this defect being closer, the corresponding MFL signal shows no return characteristic at its centre, unlike its wider counterpart in Figure 2(b). The interesting characteristic common to both signals in Figures 2(b) and 2(c) is the maximum gradient. Located close to the mean ($0.1\ T$) of each signal, the same maximum gradient (either positive or negative) is exhibited for both the wide and narrow square defects. This suggests that MFL has a maximum possible response and that this gradient represents the hypothesised band-limit of $f_H(MFL)$. Even though the gradient of the MFL signal was shown to be similar, the overall amplitude dropped. As the shape of these two defects is similar in nature, the volumetric correlations observed by [1, 5–7] are now complementary. So, based on the results presented here, perhaps the volumetric relationship noted in these publications are subject to the following conditions; defects of the same volume but different shapes are unlikely to demonstrate a volumetric relationship with the MFL signal amplitude, but, defects of the same shape but different volume may give rise to a volumetric relationship. So perhaps it is the shape of the defect that is influential and via a frequency response approach, the in-band components of MFL (and those out-of-band) can determine what shape characteristics are available and if they are, for example, attenuated.

2. Route to the MFL band-limits

Much like the examples presented in the previous section, the general approach to understanding the characteristics of MFL, is to investigate a controlled, closed-set of defects with different geometries, through either simulation or emulation. This approach has been used in a large number of publications examining the defect/MFL relationship, including [1, 2, 4, 5, 7–14]. The closed-set of defects represents a potential limitation to the investigation as a set containing all forms of defect geometries and shapes would be required. The frequency response approach aims to overcome this limitation by breaking down defects into their individual components, ultimately resulting in a map of the MFL/defect relationship.

In traditional FR analysis, conventional bandwidths are often determined by applying sinusoids to the system under investigation, for example a simple electronic amplifier. The system response is obtained by varying the input frequency of the test signal and comparing its characteristics to the signal at the output. One potential approach to achieve this is to consider the induced magnetic field (MF) component to be the input, the defect to represent system and the corresponding MFL signal as the output. Based on the conventional route, the input MF would need to be modulated with sinusoids of controlled frequencies and amplitude whilst the defect (i.e. the system) remains constant. As this employs some form of alternating mag-

netic field, time-varying parameters (e.g. velocity effects resulting in eddy currents) would be introduced. Hence, to determine the bandwidth at a fundamental level with a reduced set of variables such as time, an alternative approach is needed.

Instead, consider the defect as the input to a system which represents the induced MF (i.e. the MFL system). This reconfiguration involves 'modulating' the defects shapes themselves into sinusoids and be the input to a static magnetising field. The process is illustrated in Figure 3. whereby a steel plate with a sinusoidal defect (a) of a particular depth (%) and frequency (c/m) is passed through a simulation model of an MFL system (b) to obtain its corresponding MFL signal (c). The amplitude of (c) is then measured and is plotted with respect to the frequency of (a) on (d). This measure is represented by the cross on (d). By varying the sinusoid (a) over a range of frequencies, the amplitudes of the corresponding MFL signals (c) are then used to construct the frequency response (FR) of MFL, the green profile shown in (d).

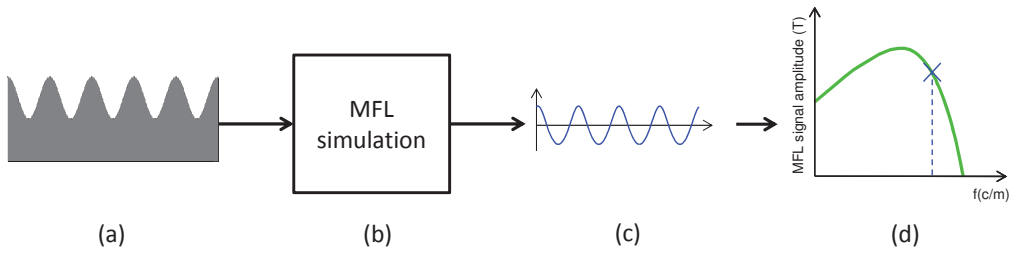

Fig. 3. Process to establish the frequency response (FR). In this work, a typical closed-set of defects are substituted with sinusoidal defects (a). When passed through a simulation (b) the amplitude of the corresponding MFL signal (c) is then plotted as a function of the sinusoidal frequency, the vertical blue line on (d). Over a range of defect frequencies the FR can be established and is represented by the green profile in (d).

While the variable parameters of the sinusoidal defects (a) are self-explanatory, the MFL system can be tailored to any configuration. For this paper, the basic setup of the MFL system (b) is as follows. Like the defect profile, a cross-section model of an MFL scanner is considered, comprising of a large coil centred around a steel plate that induces a homogeneous field in a steel plate with a uniform thickness. The MFL signal is obtained by obtaining the magnitude of magnetic flux density $|B_{XZ}^{Leak}|$ on a parallel plane that is at a fixed height of 4.1 mm from the surface of the steel plate. This culminates in a series of MFL measurements, with a spacial resolution of 0.1 mm. The peak-to-peak amplitude of the MFL signal across the steel plate is obtained from the series of $|B_{XZ}^{Leak}|$ measurements. To create the full FR, the process is repeated by changing the period of the sinusoidal defects.

Other shapes including equivalent square wave defects were considered but the sinusoidal profile is the only type that would give rise to a single frequency component. This makes comparisons in the spectral domain easier. The simulation route was also chosen because ascertaining the FR through emulation with a collection of machined cosine defects would be an exceedingly difficult task, let alone a costly one.

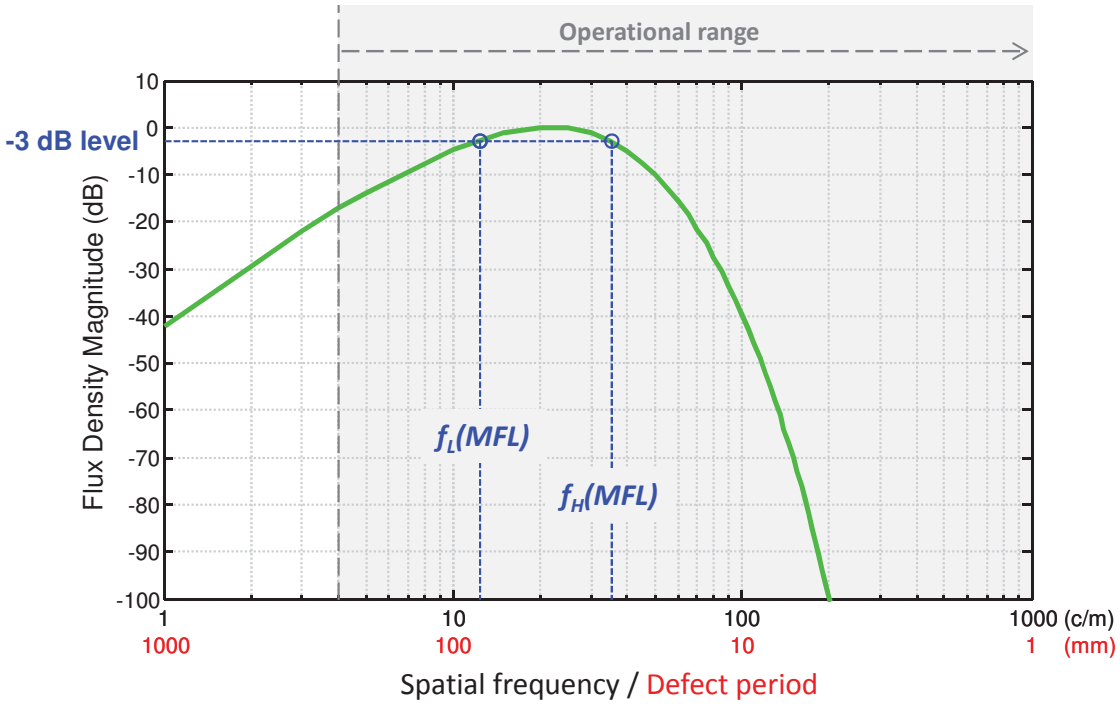

Fig. 4. Flux density magnitude ratio to input defect depth as a function of frequency. The equivalent period of the defect sinusoid δ_L is also presented on the abscissa. Because cosines are used, both defect period and defect length are the same. This Figure represents the frequency response (FR) of MFL for defects with a depth of 50 %. Normalised magnitude of corresponding MFL signal as a function of harmonic cosine defect frequency, represented as number of defect cycles per metre (c/m). The MFL bandwidth is around 23 c/m.

3. Frequency response of MFL and its bandwidth

Figure 4. depicts the amplitude of MFL as a function of defect frequency for a harmonic set of sinusoidal defects. Along with defect frequency in c/m, the equivalent period of the defect sinusoid δ_L in mm is also presented on the abscissa. Because cosines are used to derive the FR, both defect period and defect length represent the same geometry.

The lowest and fundamental frequency component of this work is 1 c/m and is presented on the left of the abscissa with the highest frequency component of 1000 c/m on the right. Though the fundamental component represents a very large defect, 1000 mm in length, the operational region of MFL above 4 c/m is also highlighted.

The FR profile presented here describes the relationship between the amplitudes of the MFL system input and its output, denoted by A_i and A_o respectively. This relationship is described by a ratio of A_o and A_i using the peak magnetic flux density magnitude and percentage of defect depth (δ_D). This is the gain ratio G in dB and is presented on the ordinate with a logarithmic scale, calculated using Equation 1.

$$G = 20 \times \log_{10}\left(\frac{A_o}{A_i}\right) = 20 \times \log_{10}\left(\frac{|B_{XZ}^{Leak}|}{\delta_D}\right) \tag{1}$$

Here, δ_D represents the depth as a percentage of material loss between 0.1 and 1 (through

hole). To reduce the number of variables, only $\delta_D = 0.5$ is used and is common to all frequencies. Other depths will be considered for further research. In addition, the FR has been DC-shifted so that its peak, located at around 30 c/m, sits at 0 dB. The primary purpose of this offset is to help illustrate the bandwidth at the -3 db point, relative to the largest MFL signal amplitude and can be achieved in practice by applying a DC offset in the electronics of the data capture system to maximise its dynamic range.

The overall FR can be seen to have a relatively band-pass characteristic with the magnitude increasing from 1 c/m up to a peak amplitude in the region of 30 c/m (corresponding to defect period of just over 33 mm). Thereafter decreasing at an ultimate rate of around $-85dB$ per decade. At the upper frequencies, defects with components smaller than 10 mm in length are heavily attenuated. A signal registered under 100 dB is thought to be a suitable limit in practice; this measure will be addressed in the next section.

The vertical blue dashed lines highlight the lower ($f_L(MFL)$) and upper ($f_H(MFL)$) cut-off frequencies, governed by a threshold of -3 dB. These limits can be represented by the notation in Equation 2.

$$BL(-3\ dB) \in [f_L(MFL), f_H(MFL)] \tag{2}$$

For this example, the in-band region of MFL spans between the band-limits of $BL(-3\ dB) \in [12, 35.5]$. Components lower than 12 c/m and greater than 35.5 c/m are, in this case, out-of-band. These band-limits equate to defects with periods between 81 mm and 28 mm when $\delta_D = 50$ %. Under these conditions the bandwidth of MFL is around 23.5 c/m. Based on this first insight into the capabilities of the MFL approach, its bandwidth can be considered surprisingly narrow.

Interestingly, the upper limit of 35.5 c/m is indicative of the comments of Ramirez [4], *"for the motion axis, there is no frequency component over* 50 Hz*"* (i.e. 50 c/m), which is then followed by the statement *"This indicates significant over sampling but at no real cost"*. Ramirez ascertained that the 50 Hz cut-off from a single defect[2] and implies that MFL is not capable of finding defects less than 9 mm in diameter and 2 mm deep, let alone sizing them. While the Nyquist criterion had been surpassed by a factor of four based on the findings of Ramirez, it did highlight the relatively low upper frequency limit of MFL, again approximated by the 35.3 c/m upper limit depicted in Figure 4. What the '50 Hz' finding reported by Ramirez did not consider is the variation in attenuation of defect components at different frequencies. It is clear in Figure 4. that frequency components above '50 Hz' do exist and are simply attenuated.

Through identifying these band-limits it is now possible to take any defect profile and identify which of its components would be in-band or out-of-band. It can also determine the level of attenuation the MFL system introduces to defects frequency components. Perhaps by knowing this, the process could be reversed and the level of attenuation normalised to reconstruct the original defect profile, assuming that the signals are within the bandwidth of MFL. However, the narrow bandwidth found appears not to reflect the defects that can be located with MFL.

[2]For a semi-spherical defect 100 mm in diameter with a depth of 2 mm and sampling every 1 mm at a speed 450 mm/s (i.e. a sample rate of 450 Hz)

3.1 A practical dynamic range

Based on the limited bandwidth of MFL now established, it can be argued that the bandwidth described at the $-3\ dB$ level does not represent the practicable capability of MFL; MFL can certainly locate defects with diameters less than 28 *mm* (35.5 c/m). As discussed in section 1., the level at which the band-limits are determined can be tailored to some standard level or to the system and its application. For an MFL system, one component that can indicate a minimum threshold is the front-end analogue to digital converter (ADC). While a threshold at $-3\ dB$ can be used to asses the relative capability of MFL; a typical MFL system may be able to comfortably record defects with harmonics of a magnitude well below this level. As an illustrative example, consider an ADC with a 10-bit resolution. The signal-to-quantisation-noise-ratio (SQNR) measure can be used to ascertain the noise floor of the ADC and hence the dynamic range. This can be calculated with equation (3) where N represents the number of bits.

$$SQNR = N \times 20 \times log_{10}(2) = N \times 6.0306\ dB \tag{3}$$

Then, for an 10-bit system, the SQNR can be calculated to be:

$$10 \times 6.0206\ dB \approx 60\ dB \tag{4}$$

This can be considered a crude estimation, as the level of magnetic noise and electrical noise is not considered in the calculation. Determining the noise characteristics on the FR and under different conditions, is an avenue for further work. However, removing 10 dB, for example, may estimate for such noise and give a more practical representation of the upper and lower cut-off. Of course, using a noise reduction approach such as detailed in [15], the SQNR may be improved. For the same conditions as the previous FR example and if a level of ADC 'bit' quantisation noise is considered, then a dynamic range of around $-50\ dB$ would be practical and be able to widen the bandwidth of MFL, reflecting defect components with the lower and upper frequency cut-off's at 0.4 c/m and 116 c/m respectively, i.e. $BL(-50\ dB) \in [0.4, 116]$. The bandwidth has now increased by nearly five fold, from 23.5 c/m to approximately 116 c/m. In this case, $f_H(MFL)$ has been increased so that defects with periods of around 8.6 *mm* with a depth of 50 % could be represented in the MFL signal. Increasing the ADC quantisation to 16-bit results in an SQNR of 96 dB meaning that the vast majority of the MFL FR would encompass defect diameters down to 5 *mm* and depths of 50 %.

From this simple example, it is clear that the proposed FR approach can be used to not only identify the capabilities and limitations of MFL itself but also guide the design of the MFL system, in this case the dynamic range of the acquisition unit.

4. Conclusion

The concept of a band-limited MFL system and its relative location within a defect space has been presented with the aim to increase the understanding of the relationship of defects to MFL. This concept and its fundamental application in fields such as audio signals naturally led to the postulation that a defect profile can be constructed from one or more frequency components. The attractive properties of this concept is its ability to describe:

- 'Defect space' (DS), a range of frequencies that can be used to describe all possible defect profile combinations,

- 'MFL signal space', a subregion of DS with band-limits that can identify the defect components that can be reflected by MFL.

Based on the band-limiting nature of MFL, a defects components could then be described as being either in-band, out-of-band or across-band and classified based on the frequency components needed to describe a defect. The derivation of these classes requires the knowledge of the band-limits of MFL, discovered with an original frequency response (FR) approach. Unlike the restricted performance measure that is normally ascertained with a closed-set of defects, the relationship between any defect and corresponding MFL signal can be described.

Derived through the creation of sinusoidal defects that can be varied in both depth and frequency, the experimental work for a simple MFL set-up shows that the FR of MFL approximates a band-pass filter; a relatively narrow one that considerable attenuates defects *mm* or even $10's$ of *mm* in diameter. The presented FR has also identified the level of attenuation over the range of defect frequencies considered and that high frequency components in particular, demonstrate the greatest level of attenuation. This is the region where defect components are out of range of the MFL signal. Practically, the narrow band-limit can be accommodated by choosing an ADC with a suitable dynamic range. Doing so will effectively widen the band-limits that can be recorded and hence locate and size smaller defects.

The proposed FR for the MFL system is arguably a simple idea, but it is believed that this approach has for the first time quantified the band-limiting nature of MFL and its ability to locate and reflect defect profiles. It maybe surprising that such an approach has not been considered before and that this work is the first case where it has been applied in the context of MFL.

This paper serves as an introduction to the FR of MFL. There are a vast number of parameters that can be investigated, the next ones to considered include the influence of defect depth (i.e. amplitude of the sinusoidal defects), surface origin of the defect and MFL system parameters such as position of the MFL measurement (i.e. height of sensors from the steel surface).

5. Acknowledgements

This work is funded by Silverwing UK Ltd. The support of Ralf Lieb at Silverwing (UK) Ltd. is also acknowledged.

6. Bibliography

References

[1] J. Qi, S. Qingmei, L. Nan, Z. Paschalis, and W. Jihong. Detection and estimation of oil-gas pipeline corrosion defects. *Proceedings of the 18th international conference on systems engineering (ICSE 2006)*, pages 173–177, 2006.

[2] S. Saha, S. Mukhopadhyay, U. Mahapatra, S. Bhattacharya, and G.P. Srivastava. Empirical structure for characterizing metal loss defects from radial magnetic flux leakage. *NDT & E International*, 43:507–512, 2010.

[3] M. Ravan, R.K. Amineh, S. Koziel, N.K. Nikolova, and J.P. Reilly. Sizing of 3-D arbitrary defects using magnetic flux leakage measurments. *IEEE transactions on magnetics*, 46(4):1024–1033, April 2010.

[4] A. R. Ramirez. Automatic classification of defects in aboveground storage tanks via magnetic flux leakage. *PhD Thesis, Swansea University*, 2009.

[5] D. H. Saunderson. The MFE tank floor scanner - a case history. *IEE colloquium on non-destructive evaluation*, 1988.

[6] P. C. Charlton and K. E. Donne. The computer modelling of magnetic flux leakage signals using the boundary element method. *32nd annual British conference on NDT*, 1993.

[7] H. Zuoying, Q. Peiwen, and C. Liang. 3D FEM analysis in magnetic flux leakage method. *NDT & E International*, 39:61–66, 2006.

[8] D. L. Atherton and M. G. Daly. Finite element calculation of magnetic flux leakage detector signals. *NDT International*, 20 (4), August 1987.

[9] P. C. Charlton. A theoretical and experimental study of the magnetic flux leakage method for the analysis of corrosion defects in carbon steel plate. *PhD Thesis, Swansea institute of higher education*, 1995.

[10] S. Lukyanets, A. Snarskii, M. Shamonin, and V. Bakaev. Calculation of magnetic leakage field from a surface defect in a linear ferromagnetic material: an analytical approach. *NDT & E International*, 36, 2003.

[11] S. Huang, L. Li, H. Yang, and K. Shi. Influence of slot defect length on magnetic flux leakage. *Journal of Materials Sciences & Technology*, 20, 2004.

[12] K. Sekine, N. Kasai, and H. Maruyama. The non-destructive evaluation method for far-side corrosive type flaws in steel plates using magnetic flux leakage technique. *15th World Conference on Non-Destructive Testing (WCNDT)*, 2000.

[13] Y. S. Su, W. Lord, G. Katragadda, and Y. K. Shin. Influences of velocity on signal responses of Magnetostatic non-destructive testing tools: a prediction from finite element analysis. *IEEE transactions on magnetics*, 30(5):3308–3311, 1995.

[14] J. Qi. Experimental study of interference factors and simulation on oil-gas pipeline magnetic flux leakage density signal. *International conference on mechatronics and automation*, 2007.

[15] A. Joshi, L. Upda, S. Upda, and A. Tamburrino. Adaptive wavelets for characterising magnetic flux leakage signals from pipeline inspections. *IEEE transactions on magnetics*, 42, 2006.